Talanta 134 (2015) 640–649

Contents lists available at ScienceDirect

Talanta

journal homepage: www.elsevier.com/locate/talanta

Trace level voltammetric determination of lead and cadmium in sediment pore water by a bismuth-oxychloride particle-multiwalled carbon nanotube composite modified glassy carbon electrode

Sandra Cerovac [a], Valéria Guzsvány [a,*], Zoltán Kónya [b,c], Amir M. Ashrafi [d,e], Ivan Švancara [d], Srđan Rončević [a], Ákos Kukovecz [b,f], Božo Dalmacija [a], Karel Vytřas [d]

[a] University of Novi Sad, Faculty of Sciences, Department of Chemistry, Biochemistry and Environmental Protection, Trg D. Obradovića 3, 21000 Novi Sad, Serbia
[b] University of Szeged, Department of Applied and Environmental Chemistry, Rerrich Béla tér 1, 6720 Szeged, Hungary
[c] MTA-SZTE Reaction Kinetics and Surface Chemistry Research Group, Rerrich Béla tér 1, 6720 Szeged, Hungary
[d] University of Pardubice, Department of Analytical Chemistry, Faculty of Chemical Technology, Studentská 573, 532 10 Pardubice, Czech Republic
[e] MemBrain, s.r.o., Pod Vinicí 87, 471 27 Stráž pod Ralskem, Czech Republic
[f] MTA-SZTE "Lendület" Porous Nanocomposites Research Group, Rerrich Béla tér 1, 6720 Szeged, Hungary

ARTICLE INFO

Article history:
Received 9 September 2014
Received in revised form
30 November 2014
Accepted 5 December 2014
Available online 13 December 2014

Keywords:
Bismuth-oxychloride/multiwalled carbon nanotubes
Bismuth/multiwalled carbon nanotubes
Modified electrodes
Lead and cadmium
Determination
Sediment pore water

ABSTRACT

Two multiwalled carbon nanotubes-based composites modified with bismuth and bismuth-oxychloride particles were synthesized and attached to the glassy carbon electrode substrate. The resultant configurations, Bi/MWCNT-GCE and BiOCl/MWNT-GCE, were then characterized with respect to their physicochemical properties and electroanalytical performance in combination with square-wave anodic stripping voltammetry (SWASV). Further, some key experimental conditions and instrumental parameters were optimized; namely: the supporting electrolyte composition, accumulation potential and time, together with the parameters of the SWV-ramp. The respective method with both electrode configurations has then been examined for the trace level determination of Pb^{2+} and Cd^{2+} ions and the results compared to those obtained with classical bismuth-film modified GCE. The different intensities of analytical signals obtained at the three electrodes for Pb^{2+} and Cd^{2+} vs. the saturated calomel reference electrode had indicated that the nature of the modifiers and the choice of the supporting electrolyte influenced significantly the corresponding stripping signals. The most promising procedure involved the BiOCl/MWCNT-GCE and the acetate buffer (pH 4.0) offering limits of determination of 4.0 μg L^{-1} Cd^{2+} and 1.9 μg L^{-1} Pb^{2+} when accumulating for 120 s at a potential of −1.20 V vs. ref. The BiOCl/MWCNT electrode was tested for the determination of target ions in the pore water of a selected sediment sample and the results agreed well with those obtained by graphite furnace atomic absorption spectrometry.
© 2014 Elsevier B.V. All rights reserved.

1. Introduction

The trace determination of Cd^{2+} and Pb^{2+} with different metallic-film electrodes that now often replace toxic mercury based electrodes is a challenge in many electroanalytical laboratories [1–3]. One of the first examples of this kind is the bismuth-film electrode (BiFE) in combination with anodic stripping voltammetry (ASV) [1] that has been introduced nearly fifteen years ago and, since then, becoming apparently the most popular working electrodes due to its environmentally friendly character. The ability of bismuth to form intermetallic alloys with different elements, as well as its insensitivity towards dissolved oxygen are just some of remarkable electrochemical features of bismuth-based electrodes that stay behind their widespread use [4,5].

Up until now, many types of bismuth-film or bismuth modified electrodes have been proposed and most of them also proven to be useful for different target analytes, first of all, for selected metals at the very low concentration level [1,6–31], but also for various organic compounds [32–38], in batch [1,6–25,29–31] and in flow injection [26–28] working regimes. Carbon-based electrode materials are well-known substrates for modification with bismuth as glassy carbon [1,9,13], carbon paste [7,8,12,17,18,29,30] and boron-doped diamond [10,11], but some metal electrodes like gold [19,22], platinum [13] and silver-amalgam [35] are convenient for modification with bismuth, too. In fact, bismuth-based configurations represent a specific type of chemically or physically modified electrodes that can be obtained by various methods, ranging from simple electrodeposition, via the adding of various Bi^{3+}

* Corresponding author. Tel.: +381 21 485 2740; fax: +381 21 454 065.
E-mail address: valeria.guzsvany@dh.uns.ac.rs (V. Guzsvány).

http://dx.doi.org/10.1016/j.talanta.2014.12.002
0039-9140/© 2014 Elsevier B.V. All rights reserved.

compounds (e.g.: Bi_2O_3 [18], BiF_3 [29] or NH_4BiF_4 [30], etc.) as bulk-modifiers, up to the preparation of templates by screen-printing [26,27,39] and sputtering [31], etc.

Different designs were elaborated to improve the adhesion of bismuth particles onto / into the substrate, especially those based on carbonaceous materials, which expands the applicability of the respective electrodes at various pH, or to enhance the stability, sensitivity and/or selectivity of the electrode surface [40–52]. There were numerous efforts to improve the sensitivity of bismuth-based working electrodes, including the expansion of the sensor surface via the synthesis of mesoporous bismuth-based materials [41,42], the enlargement of the substrate electrode surface before modification with bismuth [43] and the incorporation of micro/nanoparticles of bismuth or bismuth-composite nanoparticles [20,44–53]. Nafion® protective layers [15,20,21,23–25,27,48,51], or other compounds like surfactants [15,21] or complex-forming agents (e.g. α,α′-bipyridyl [25], crown ethers [27] etc.) were found to improve the sensitivity and/or selectivity of the methods.

Multiwalled carbon nanotubes (MWCNTs), especially in their functionalized forms, are widely used as building blocks of electrodes because of their unique electrical conductivity, large surface area, and high affinity towards certain target analytes. It is well-known that bismuth-modified carbon nanotube-based electrodes are excellent with respect to electrochemical detection of ultratrace metals [45–52]. Also, it is known that the combining MWCNTs with Bi_2O_3 gives rise to composites appropriate as the modifiers of choice for the determination of H_2O_2 [44], anticoagulant acenocoumarole [53] and antidepressant drug escitalopram [54], as well.

Electrochemical techniques have often been used to study environmental processes related to water and sediment quality either in the field or in the laboratory [10,55–63]. Frequently measured target analytes are usually various elements, such as Fe, Mn, Cr, Co, Pb, etc., and sulphur or phosphorus in its different form in the water as well as in the sediment samples. Related to the sediment characterization is the “sediment pore water” (or also “interstitial water”) whose quality is being considered as important parameter, indicating the actual processes/equilibria between the sediment and bulk water phases [64].

In the present work, we have combined the benefits of bismuth-based modifiers, BiOCl/MWCNT and Bi/MWCNT, with the outstanding electronic properties of MWCNT enhancing the sensitivity of the traditional BiFE based anodic stripping voltammetric method for the determination of toxic heavy metal ions, namely: Pb^{2+} and Cd^{2+}. Finally, the methodical procedure intended for the trace analysis was optimized with both types of electrodes, being compared with the BiF-GCE. The applicability of the method was tested on the determination of both Cd^{2+} and Pb^{2+} in the pore water of a real sediment sample from the river basin Great Backa Canal (Veliki Bački Kanal, R. Serbia). In the case of pore water sample, comparative graphite furnace atomic absorption spectrometric (GF-AAS) measurements were performed.

2. Experimental

2.1. Chemicals

Analytical grade *N*,*N*-dimethylformaldehyde (DMF), Nafion® (wt. 5%), $NaBH_4$, NH_3OHCl, CH_3COONa, cc. HCl and cc. CH_3COOH were purchased from Merck (Darmstadt). The multiwalled carbon nanotubes used in this study were synthesized from ethylene using chemical vapor deposition over Co–Fe/alumina catalyst. ICP stock solutions (all in concentration of 1000 ± 1 mg L^{-1}) of Bi^{3+}, Pb^{2+}, Cd^{2+}, and $BiCl_3$ were purchased from Sigma Aldrich. The sediment was sampled from the Great Backa Canal (R. Serbia).

2.2. Methods

An Autolab electrochemical analyzer operated via the GPES 4.9 software (Metrohm Autolab, Utrecht, The Netherlands) was used for all electrochemical measurements. The cell stand included a three-electrode system with GCE (⌀ 3 mm, Amel, Italy) substrate electrode surface modified with BiOCl/MWCNT, Bi/MWCNT or BiF as working, a platinum wire (Amel) as auxiliary electrode and a saturated calomel electrode as a reference.

Powder X-ray diffraction (XRD) patterns for the synthesized materials were obtained using a Rigaku Miniflex II instrument using Cu *K*α radiation. Surface morphology characterization and semi-quantitative chemical analysis of the BiOCl/MWCNT and Bi/MWCT nanomaterials were performed in a HITACHI S-4700 Type II cold field emission scanning electron microscope with an integrated Röntec QX2 EDS detector.

A graphite furnace atomic absorption spectrometer (Perkin Elmer Aanalyst 700) was applied for comparative sediment sample analysis. A Sonorex digitec (Bandelin) ultrasonic bath was used for the synthesis of bismuth-based materials and an ISCRA centrifuge for the separation and washing steps of the synthesized composite materials.

All pH measurements were made using a digital pH-meter (Radiometer, Nederland) and a combined glass electrode (Jenway, England).

2.3. Working electrode material preparation

2.3.1. BiOCl/MWCNT and Bi/MWCNT electrodes

The BiOCl/MWCNT-GCE and Bi/MWCNT-GCE were prepared *ex situ* by simple drop-coating of the appropriate suspensions of target modifiers on the freshly polished glassy carbon electrode surface. The synthesis of modifier materials is based on our recently published procedure of Sb/MWCNT preparation with $NaBH_4$ reduction and surface coating [65]. Briefly, in the case of both composites $BiCl_3$ (20 mg), MWCNT (16.4 mg) and 5%Nafion® solution (100 μL) were dispersed in DMF (10 mL) using an ultrasonic bath for 30 min. For Bi/MWCNT, 0.25 mL of a freshly prepared 1.8 mol L^{-1} aqueous solution of $NaBH_4$ was added to the dispersion and stirred for 10 min, while in the case of BiOCl/MWCNT 0.25 mL of 1.8 mol L^{-1} NH_3OHCl was added. The solid part was precipitated using a centrifuge (600 rpm for 15 min) and decanted. The precipitate was washed with ethanol (2 ×) and acetone (1 ×), and then transferred to a hot air oven and dried at 220 °C for 20 min. 0.5 mg from each sample was dispersed in a mixture of ethanol (0.9 mL) and Nafion®0.5% (0.1 mL), and sonicated for 20 min. 5.0 μL aliquots of the resulting suspensions were dropped on the glassy carbon electrode surfaces and dried at room temperature.

2.3.2. Bi particles

The Bi nanoparticles were obtained using the Bi/MWCNT synthesis procedure but without adding any nanotubes. The obtained particles served for the comparison of XRD characteristics.

2.3.3. BiF-GCE

A cell containing the aqueous solution of a Bi^{3+} (0.50 mg L^{-1} in acetate buffer at pH 4.0) was electrolyzed under continuous stirring at the cathodic potential of −1.20 V for 120 s similarly as was elaborated earlier [1].

2.4. Experimental procedures

2.4.1. Voltammetric measurements

For the basic electrochemical characterization of the Bi/MWCNT and BiOCl/MWCNT modified GCEs cyclic voltammetric experiments were performed in acetate buffer and hydrochloride solutions (pH 4.0 and 2.0) in the potential range from 0.30 V to −1.20 V (with negative ongoing direction) at 50 mV s^{-1} scan rate. SWASV measurements in the model systems were performed in both supporting electrolytes by injecting predetermined volumes of Pb^{2+} and Cd^{2+} standard solutions with a micropipette. Optimizations were performed with respect to accumulation potential (E_{acc}, from −0.80 V to −1.40 V) and time (t_{acc}, from 60 s to 600 s). The optimized process corresponded to applying a deposition potential of −1.20 V for an accumulation time of 120 s while the solution was stirred. The SW voltammograms were recorded after an equilibrium period of 10 s. The electrode surface was treated electrochemically by applying a potential more positive than the oxidation potential of the analytes, i.e., at 0.30 V for 30 s after each measurement. In the case of real sample analysis, pore water from the sediment sample was injected instead of a standard solution (3.0 mL of pore water and 7.0 mL of acetate buffer pH 4.0). The measurement procedure itself was very similar to that of the model solutions except that an accumulation time of 900 s was applied and the signals were recorded on BiOCl/MWCNT-GCE. In real sample analysis the standard addition method was used for the identification and quantification of the target analyte(s).

2.4.2. Scanning electron microscopy

The SEM measurements were performed with the accelerating voltage of 20 kV. Bi/MWCNT and BiOCl/MWCNT samples were investigated directly, i.e., without any sample preparation steps.

2.4.3. X-ray diffraction measurements

Four different samples: the original MWCNT, Bi NPs, Bi/MWCNT and BiOCl/MWCNT were characterized in the range from 0° to 80° 2Θ.

2.4.4. GF-AAS, USEPA method 7010

Comparative measurements were performed as follows: a sample aliquot was injected into the graphite tube of the furnace, evaporated to dryness, charred and atomized. The content of metal (s) was determined directly from the read-out system of the instrument.

2.4.5. Real sample pretreatment

The sediment from the Great Backa Canal was sampled with an Ekman bottom grab sampler at one selected location. The sample treatment was performed as follows: the sediment was centrifuged at 3000 rpm for 12 min to separate the pore water. The pore water was then acidified with cc. HNO_3 to pH < 2 for conservation and for GF-AAS measurements. Voltammetric measurements were performed on unfiltered sampes adjusted to pH 4.0 by the acetate supporting electrolyte immediatly prior to measurement(s).

3. Results and discussion

3.1. Physical characterization of the BiOCl/MWCNT and Bi/MWCNT composites

Bi/MWCNT and BiOCl/MWCNT composites were characterized by SEM and XRD. Fig. 1A and B shows micrographs of the composite material synthesized with reducing agent $NaBH_4$, while parts C and D characterize the composite prepared in the presence of NH_3OHCl. MWCNT fibers can be recognized as the skeleton of the composite in both cases. However, there are significant

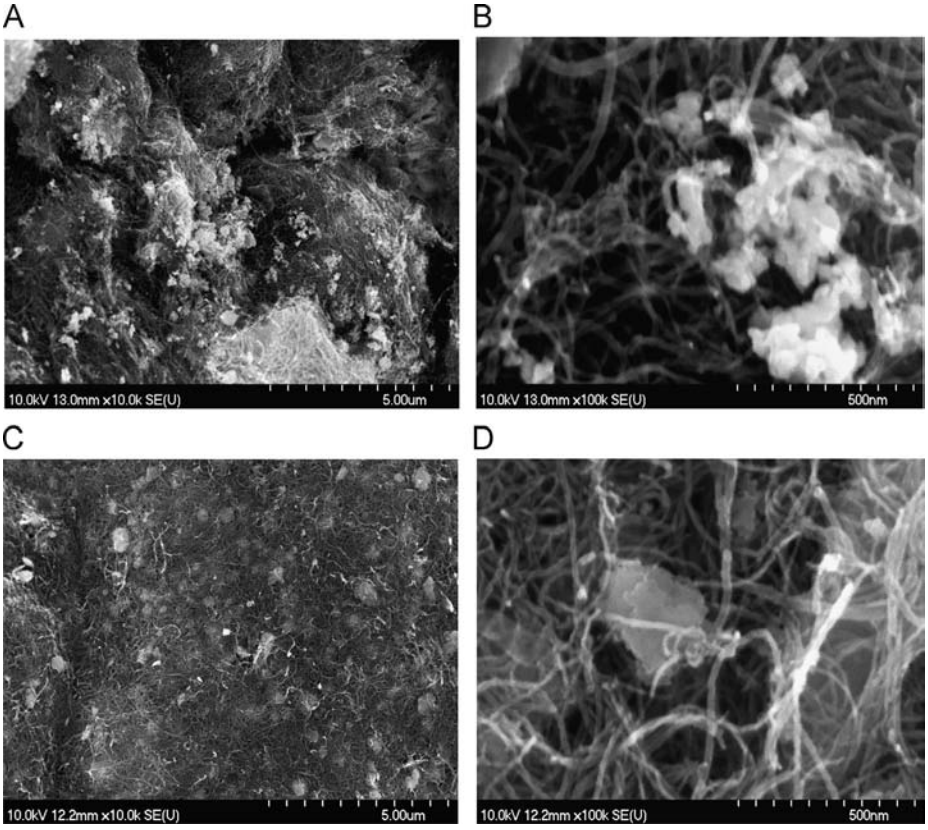

Fig. 1. SEM micrographs of Bi/MWCNT (A and B) and BiOCl/MWCNT (C and D).

differences between the two materials in the differing morphology of the bismuth-containing particles. The composite obtained by the reduction of Bi^{3+} with $NaBH_4$ is characterized by nuclei that are densely and randomly distributed over the MWCNT fibers. Their apparent primary diameter is 50–100 nm but they can aggregate into significantly larger particles. On the other hand, the composite obtained in the presence of NH_3OHCl exhibits a more uniform size distribution of bismuth-containing particles measuring with 100–300 nm in diameter. Based on Fig. 1D, it can be proposed that the MWCNT fibers surround the bismuth-containing particles and entrap them in the nanotube framework.

Line profiling energy dispersive X-ray spectroscopy (EDS) performed on both composites (not shown here) revealed that (i) their overall composition was approximately 20% bismuth and 65% of carbon and that (ii) the individual particles consisted of bismuth and oxygen. Local oxygen enrichments (up to 30%) were identified in the nanoparticles attached to the nanotubes. This phenomenon was more pronounced in the material obtained by NH_3OHCl treatment.

The X-ray diffractograms in Fig. 2 show the characteristic diffraction patterns of the synthesized materials: MWCNT (A), Bi (B), Bi/MWCNT (C) and BiOCl/MWCNT (D). The aim of the XRD measurements was to characterize the bismuth-rich phase formed and to determine the possible impact of this phase on the composites by means of identifying the types of the bismuth-based particles. The XRD patterns for all MWCNT-based materials revealed the presence of a broad peak at 25.8° corresponding to the interlayer spacing (0.34 nm) of the nanotubes (d_{002}) in good agreement with the literature [66]. The XRD pattern of the Bi sample, synthesized from Bi^{3+} by $NaBH_4$ reduction exhibits easily recognizable sharp peaks at 27.1; 37.9; 39.6; 46; 48.7; 56.1; 62.2; 64.6°. These reflections can be readily indexed to the pure rhombohedral phase of bismuth (JCPDS 05-0519). The XRD pattern also indicates that the samples are phase pure and lack any remnants (such as e.g. bismuth-hydroxide). The MWCNT composite material obtained by $NaBH_4$ treatment features an XRD pattern (Fig. 2C) that combines the signals of MWCNT and Bi and presents a recognizabe impurity (or low amount) of tetragonal BiOCl (see the discussion for Fig. 2D). It can be concluded that this composite material integrates two main components: (i) multiwalled carbon nanotubes and (ii) rhombohedral Bi; therefore, it was named as Bi/MWCNT (when the BiOCl can be removed by washing in appropriate acidic media). On the other hand, in the case of NH_3OHCl treatment the composite XRD peak positions (Fig. 2D) were as follows: 11.9; 24.2; 25.8; 32.6; 33.5; 36.6; 41.0; 46.8; 49.7; 54.3; 55.2; 58.7;60.6;63.0;68; 74.8°. Thus, the crystalline modifier phase can be well indexed to the tetragonal structure of BiOCl (JCPDS 06-0249).

3.2. Electrochemical characterization of Bi/MWCNT and BiOCl/MWCNT modified glassy carbon electrodes

The comparative cyclic voltammograms (CV), shown in Fig. 3, were recorded on Bi/MWCNT-GCE (A) and BiOCl/MWCNT-GCE (B) in different supporting electrolytes, 0.01 mol L^{-1} HCl, pH 2.0 (curve 1), and acetate buffer solution pH 4.0 (curve 2).

In the potential range investigated, the peak potential difference (see Table 1) corresponds to the irreversible redox transformation of bismuth-based modifiers present in the composite.

Moreover, the splitting of reduction peaks (with different shapes) was observed with both electrodes in the acetate buffer solution. Peak shapes and intensities indicate that the BiOCl/MWCNT and Bi/MWCNT modifiers have different electrochemical properties, which can be explained by the different fundamental characteristics of the main bismuth-containing particles. The current signals obtained by BiOCl/MWCNT-GCE were ca. two-times higher than those recorded on the Bi/MWCNT-GCE configuration. In the case of HCl used as the supporting electrolyte, the reduction peaks were more pronounced than the oxidation signals, while in the acetate buffer, the peak characteristics were almost the same.

Reduction potentials summarized in Table 1 define the effective range of electrodeposition of Cd^{2+} and Pb^{2+} target analytes, while the oxidation part of the CVs revealed the operation range of the sensors as well as their possible cleaning potentials.

3.3. Comparison of BiOCl/MWCNT and Bi/MWCN modified glassy carbon electrodes

The differences between the sensor surfaces of Bi/MWCNT (A) and BiOCl/MWCNT (B) modified glassy carbon electrodes were recognizable from the test SWASV responses of Pb^{2+} and Cd^{2+} in the above mentioned two supporting electrolytes (Fig. 4).

As first, the Bi/MWCT-GCE was applicable in both investigated media, exhibiting higher Cd^{2+} signals in HCl supporting electrolyte, but – in general – with lower current intensities for both target analytes compared to those obtained with the BiOCl/MWCNT-GCE at pH 4.0. While both electrodes were applicable in acetate buffer, in HCl solution the BiOCl/MWCNT-GCE showed unfavorable behavior as indicated by the target analyte reoxidation signals. Namely, the Pb^{2+} determination (Fig. 4B, curve 1) is hampered because of the asymmetric shape of the oxidation peak, whereas in the case of Cd^{2+} the signal intensities are too low. The most pronounced analytical signals were observed using BiOCl/MWCNT-GCE in acetate buffer supporting electrolyte (Fig. 4B, curve 2), and these signals were around three times higher than the ones obtained on Bi/MWCT-GCE in the same electrolyte. The chemical difference in the type of bismuth modifiers is reflected in the SWASV measurements. Namely, protons from the HCl solution at pH 2.0 can chemically interact with BiOCl, which can eventually lead to the leaching of the modifier from the surface. The second phenomenon expected takes place in the accumulation step of SWASV procedure: at negative potentials (e.g. −1.2 V vs. ref.), the simultaneous enactment of different reduction processes can be expected; namely, the reduction of Bi^{3+} and target analyte ions, together with possible competitive reduction of H^+ to hydrogen evolution in the form of bubbles that have been reported to be able of attacking the bismuth-film and its compact morphology, having thus negative effect upon the overall accumulation process [4,12], including the deposition of the target metals themselves. On the other hand, BiOCl is chemically more stable at pH 4.0, and in the electrodeposition/accumulation step of SWASV procedure its electrochemical reduction will take place (see the bismuth reoxidation signal in the stripping step) together with simultaneous reduction of the target analytes Pb^{2+} and Cd^{2+}, without significant reduction of the H^+ species. In this case, the target analytes can be incorporated into the *in situ* formed bismuth lattice with a higher probability.

The target analytes might be incorporated with a different mechanism into Bi/MWCNT-GCE than into BiOCl/MWCT-GCE. Here, mostly Bi nanoparticles are formed on the carbon nanotube skeleton by chemical reduction before the electrochemical measurement; therefore, Pb^{2+} and Cd^{2+} can be electrodeposited mainly in the form of typical surface layers of bismuth. This could saturate the sensor surface at lower concentrations than in the case of the BiOCl/MWCT-GCE. Basically, the BiOCl impurity in the Bi/MWCNT composite can somehow enhance the analytical signals of Pb and Cd in the acetate buffer-based supporting electrolyte, in accordance with the above considered mechanism, but its low amount makes this phenomenon much less pronounced. This is also evident from Fig. 4, comparing both Pb- and Cd-signals obtained with Bi/MWCNT-GCE and BiOCl/MWCNT-GCE.

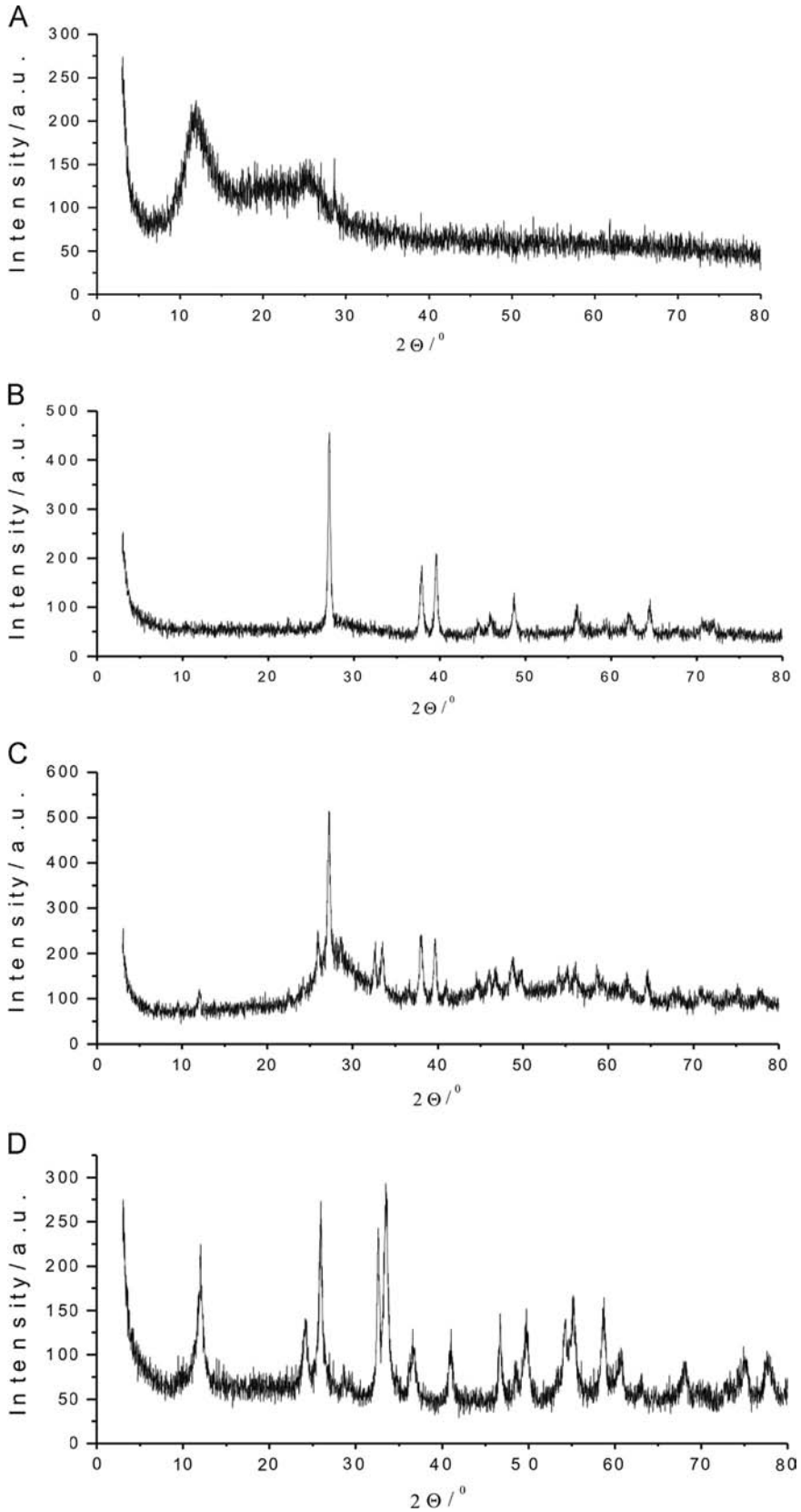

Fig. 2. XRD patterns of MWCNT (A), Bi (B), Bi/MWCNT (C) and BiOCl/MWCNT (D).

In order to compare the analytical performance of the BiOCl/MWCNT and Bi/MWCNT modifiers with that of the (traditional) BiF-GCE, all three electrodes were combined with SWASV, when the respective measurements were performed in acetate buffer (pH 4.0) containing the same concentration of both target analytes: 10 μg L^{-1}. It has been found that the most pronounced analytical signals were obtained with the BiOCl/MWCNT-GCE, followed by the performances of the Bi/MWCNT-GCE and

BiF-GCE; the last named exhibiting a half sensitivity towards both target metals compared to the first one. This finding has underlined the importance of *in situ* incorporation of the target analyte into the bulk of bismuth lattice, as well as the significance of the enlarged surface area thanks to the presence of MWCNTs.

3.4. Optimization of the stripping parameters for Bi/MWCNT-GCE and BiOCl/MWCNT-GCE

In addition to the investigations concerning the optimal supporting electrolyte type, two key parameters: the electrodeposition potential (E_{acc}) and time (t_{acc}) were studied in the case of both electrodes. Typical curves obtained in the supporting media of choice are presented in Fig. 5, together with the respective experimental conditions given in the legend(s) and with the corresponding plots in the insets.

Regarding the accumulation potential, E_{acc}, its optimal values was set to −1.20 V vs. ref., when both Cd- and Pb- signals were fairly developed, their current intensities well evaluable, and the distortion effect of eventual hydrogen evolution still not so pronounced.

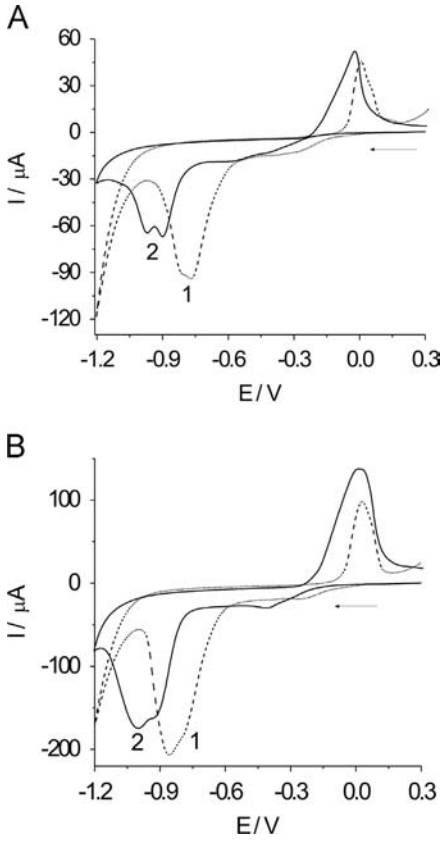

Fig. 3. Cyclic voltammograms of the developed Bi/MWCNT-GCE (A) and BiOCl/MWCNT-GCE (B) electrodes in 0.01 mol L^{-1} HCl (1) and acetate buffer pH 4.0 (2) solutions, scan rate 50 mV s^{-1}.

To optimize accumulation time, t_{acc}, the voltammograms of 30 μg L^{-1} of both target ions were recorded after different deposition times—between 60 s and 600 s. Herein, it should be noted that even highest t_{acc} values would have been possible for both new electrodes, thereby the overall signal-to-noise ratio and sensitivity could be further improved.

3.5. Comparison of the analytical performance of the developed electrodes

The concentration dependence of the electrochemical signal was studied with the optimized SWASV methods for both target analytes (Fig. 6) using BiOCl/MWCNT-GCE, Bi/MWCNT-GCE and BiF-GCE electrodes in the appropriate buffer solutions. In the case of BiOCl/MWCNT-GCE and BiF-GCE the acetate buffer pH 4.0 was applied, while in the case of Bi/MWCNT-GCE the application media was extended to the hydrochloric acid pH 2.0. The corresponding voltammograms are shown in Fig. 6 in the concentration range from 5.0 μg L^{-1} to 50.0 μg L^{-1} for both target ions, while the appropriate

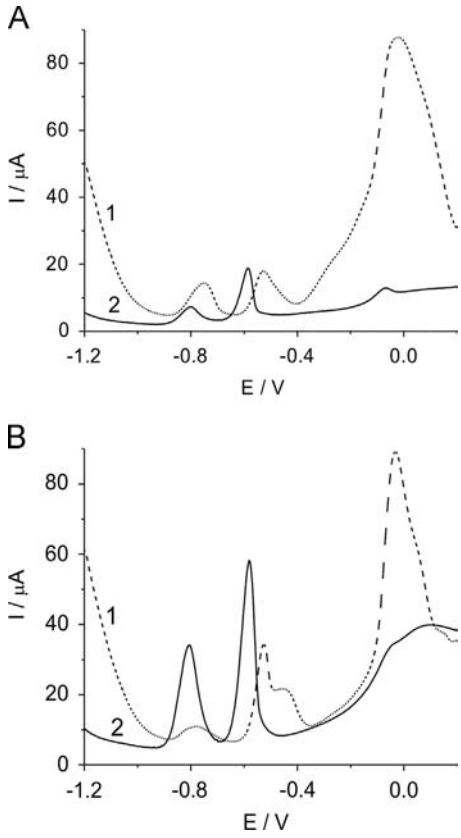

Fig. 4. SWASV signals of 50 μg L^{-1} of Pb^{2+} and Cd^{2+} recorded on Bi/MWCNT-GCE (A) and BiOCl/MWCNT-GCE (B) in hydrochloric acid solution pH 2.0 (curves 1) and acetate buffer solutions pH 4.0 (curves 2). Voltammetric measurement parameters: E_{acc} −1.20 V, t_{acc} 120 s, equilibration period of 10 s, stripping scan with a frequency of 25 Hz, potential step of 4 mV, and amplitude of 25 mV.

Table 1
Cyclic voltammetric behavior of Bi/MWCNT-GCE and BiOCl/MWCNT-GCE in acetate buffer (pH 4.0) and hydrochloride (pH 2.0) supporting electrolytes.

Supporting electrolyte	Electrodes			
	Bi/MWCNT-GCE		BiOCl/MWCNT-GCE	
	E_a [V]	E_c [V]	E_a [V]	E_c [V]
Hydrochloride acid, pH 2.0	0.01	−0.78	0.03	−0.85
Acetate buffer, pH 4.0	−0.02	−0.90 and −0.97	0.02	−0.92 and −1.00

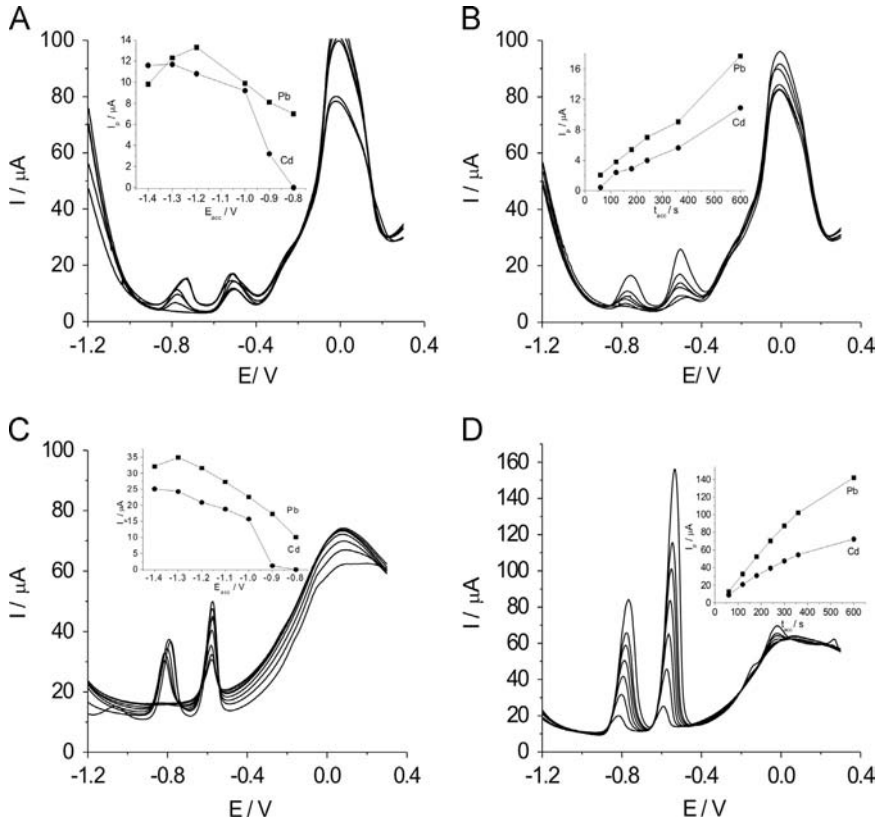

Fig. 5. Simultaneous optimization of E_{acc} and t_{acc} on Bi/MWCN-GCE (A and B) and BiOCl/MWCNT-GCE (C and D). Effect of: (A and C) deposition potential upon the stripping voltammetric response of 50 μg L^{-1} Pb^{2+} and Cd^{2+} at deposition time of 120 s and (B and D) deposition time upon the stripping voltammetric response of 30 μg L^{-1} Pb^{2+} and Cd^{2+} at deposition potential of −1.20 V. Supporting electrolytes: (A and B) 0.01 mol L^{-1} HCl (pH 2.0), and (C and D) acetate buffer (pH 4.0). The other square-wave voltammetric parameters were identical with those in Fig. 4.

analytical parameters of the methods are elaborated in Table 2. The limits of detection (as 3σ) and quantification (as 10σ) for both analytes were evaluated in the case of all investigated electrodes.

It is obvious that all of the discussed electrodes are conveniently applicable in acetate buffer solution at pH 4.0 for the trace level determination of Pb^{2+} and Cd^{2+}, while the Bi/MWCNT-GCE can serve as appropriate sensor at pH 2.0 as well, although the signals are not as intense as in the case of BiOCl/MWCNT-GCE at pH 4.0.

The repeatability of the BiOCl/MWCNT-GCE response was assessed by consecutively repeating the same SWASV measurement six times at the concentration level of 30 μg L^{-1} for both analytes and based on the appropriate I_p values the relative standard deviation (RSD) was evaluated. The RSD of the analytical signal for Pb^{2+} was 2.9%, and for Cd^{2+} 3.1%. The quality control of the synthesized BiOCl/MWCNT was performed by SWASV measurements spanning the 5–50 μg L^{-1} concentration range. Comparing the slopes of the calibration curves obtained for Pb^{2+} and Cd^{2+}, by GCE surface modified with BiOCl/MWCNTs from the repeated synthesis of the composite, reveals that their appropriate ratios did not exceed 1.2 which implicated a high level of reproducibility of MWCNT modification with BiOCl for electrode design.

Having in mind the above, because of its higher sensitivity, BiOCl/MWCNT-GCE was selected for the further analytical measurements.

3.6. *Application of the BiOCl/MWCNT-GCE for the determination of lead and cadmium in the pore water of a selected sediment sample*

The applicability of the new BiOCl/MWCNT modified GC electrode was demonstrated in the analysis of pore water obtained from sediment collected from one sampling point of the Great Backa Canal (Fig. 7). The SWASV method to determine Pb^{2+} and Cd^{2+} in the sample chosen was optimized concerning the amount of sample as well as the voltammetric procedural protocol. Besides the assesment on the performance of the electrode proposed, this analysis performed in parallel with a reference method (by GF-AAS; see below) could also reveal possible interferring species, mainly, the Cu^{2+} ions (being usually suppressed by adding either Ga^{3+} or SCN^- [4,5]). By using the optimized method with a 900 s accumulation time in the SWASV, a metal content of 27.7 ± 5.3 (n=3) μg L^{-1} Pb^{2+} was found. This result agrees within the data obtained by the GF-AAS method (25.5 ± 4.4 (n=3) μg L^{-1}). Cd^{2+} concentration in the pore water of sediment was found to be below the corresponding LOD of the examined voltammetric as well as reference GF-AAS (LOD 0.15 μg L^{-1}; LOQ 0.30 μg L^{-1}) methods. It is important to note that the proportionally increasing reoxidation peaks of Cd obtained by the three consecutive additions of standard solution which contained both target metal ions to the investigated sample in the voltammetric cell (curves 3–5) indicated that the matrix did not suppressed the analytical signal of Cd^{2+}. Finally, the above-commented agreement of the results between the voltammetric and GF-AAS analyses along with this finding on detectability of Cd^{2+} ions suggest one, that there has been no negative effect from matrix.

Furthermore, the measurements performed have indicated the presence of Pb^{2+} at a very low concentration (ultra trace level) in this sediment pore water sample. The classification of sediment quality is largely based on the assumption that the primary toxicity of its contaminants is associated with their concentration in the pore water which is their generally assumed main route of exposure [64]). In this respect, the sediment sample from the mentioned location in its actual form concerning the Pb^{2+} and Cd^{2+} content in pore water not belong to the harmful classes of sediments.

The maximum tolerated residue limit in sediment samples in the Republic of Serbia is 310 mg kg^{-1} for Pb and 6.4 mg kg^{-1} for

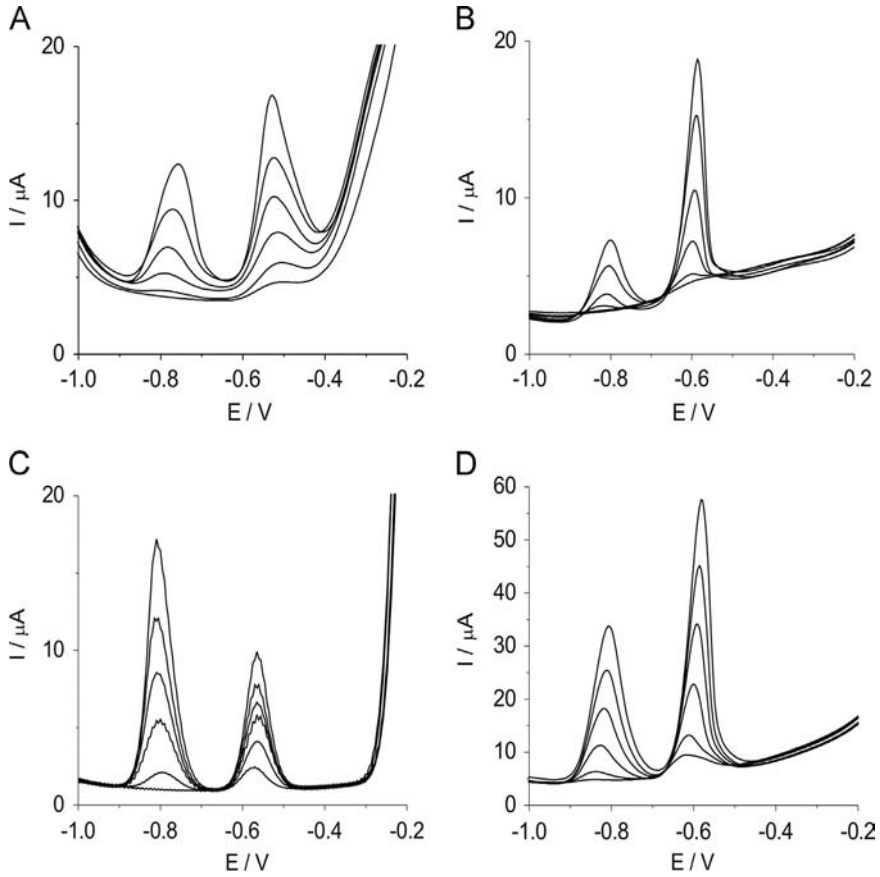

Fig. 6. Square wave anodic stripping voltammograms for increasing concentration of Pb^{2+} and Cd^{2+} under optimized experimental conditions and successive additions of Pb^{2+} and Cd^{2+} in concentration range from 5 μg L^{-1} to 50 μg L^{-1} obtained on Bi/MWCNT-GCE (A and B), BiF-GCE (C) and BiOCl/MWCNT-GCE (D) in different supporting electrolytes: hydrochloric acid pH 2.0 (A), and acetate buffer solution pH 4.0 (B–D). E_{acc} −1.20 V, and t_{acc} 120 s. Other square-wave voltammetric parameters as was described at Fig. 4.

Table 2
Comparison of analytical parameters of Pb^{2+} and Cd^{2+} determination obtained by BiOCl/MWCNT-GCE, Bi/MWCNT-GCE and BiF-GCE.

Parameters	Electrodes							
	BiF-GCE (acetate)		Bi/MWCNT-GCE (HCl)		Bi/MWCNT-GCE (acetate)		BiOCl/MWCNT-GCE (acetate)	
	Pb^{2+}	Cd^{2+}	Pb^{2+}	Cd^{2+}	Pb^{2+}	Cd^{2+}	Pb^{2+}	Cd^{2+}
Investigated concentration range [μg L^{-1}]	5–50	10–50	10–50	10–50	10–50	10–50	5–50	5–50
Slope [μA L $μg^{-1}$]	0.137	0.374	0.267	0.223	0.231	0.183	0.908	0.496
Correlation coefficient	0.986	0.992	0.999	0.996	0.999	0.996	0.998	0.988
LOD [μg L^{-1}]	1.4	5.2	2.1	2.4	1.9	3.1	0.57	1.2
LOQ [μg L^{-1}]	4.6	9.9	6.9	7.9	6.3	10.2	1.9	4.0
RSD [%]	2.1	2.7	3.3	2.9	3.4	3.5	2.9	3.1

Cd [67]. The detailed analysis of the total lead content in the same sediment sample confirmed that 45 mg kg^{-1} was actually found. This is far (about 7 times) lower than the allowed maximum residue limit. In the case of total analysis of Cd, its concentration was in the region of legally allowed range. Summarizing, the pore water analysis of sediments by appropriate high sensitivity sensor-based SWASV offers a fast method to make the first screening about the conditions/equilibriums between the pore water of sediment and the bulk water body.

Realizing the application potential of the newly designed BiOCl/MWCNT-GCE for trace level determination of Pb^{2+} and Cd^{2+}, further exploratory work is planned for the broadening of its usage for the trace level analysis of different target pollutants in complex matrices.

4. Conclusions

We have reported on the preparation and characterization of two surface modifiers, Bi/MWCNT and BiOCl/MWCNT for glassy carbon substrate electrodes. Optimization of key measurement parameters (electrodeposition time and potential, and supporting electrolyte nature) and practical application of the Bi/MWCNT-GCE and BiOCl/MWCNT-GCE configurations were investigated in detail. The analytical performance of the new electrodes was compared with a traditional bismuth-film electrode (BiF-GCE). The electrodes exhibited attractive electroanalytical performance in the determination of Pb^{2+} and Cd^{2+} in acidic media (especially at pH 4.0) when using the SWASV method. In comparison with BiF-GCE and with Bi/MWCNT-GCE, the BiOCl/MWCNT-GCE has shown

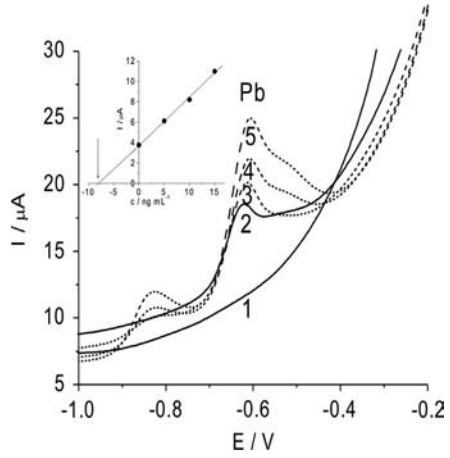

Fig. 7. BiOCl/MWCNT-GCE based SWASVs of: supporting electrolyte solution (curve 1) after addition of pore water sample (curve 2) and after consecutive standard addition of Pb^{2+} and Cd^{2+} (5 μg L^{-1}, 5 μg L^{-1} and 5 μg L^{-1}, curves 3–5, respectively). Inset is the corresponding analytical curve for Pb^{2+} determination. Other experimental parameters: t_{acc} 900 s, E_{acc} −1.20 V, square-wave voltammetric parameters as at Fig. 4.

a significant signal enhancement, which was attributed to the high specific surface area and the *in situ* generation of Bi particles from BiOCl. The new electrode design is convenient for the detection and determination of Cd^{2+} and Pb^{2+} target analytes from sediment pore water samples. This method can serve a screening tool for obtaining information about actual equilibria between pore water and the bulk water body of the river. The obtained results were in good agreement with those obtained by GF-AAS. Our research will continue to modify and improve the analytical performance of the electrodes proposed herein and in order to broaden their practical applicability.

Acknowledgement

The financial supports of the CEEPUSIII network (CIII-CZ-0212-06-1213) and the University of Pardubice under the SGFChT06 project are acknowledged, as well as the support of European Union project (Project HUSRB 1002/214/188 MATCROSS Development of new materials for application in environmentally friendly technologies for the cost effective remediation of contaminated sites threatening cross border regions). The financial support of the Hungarian Scientific Research Fund (OTKA NN 110676) and TÁMOP-4.2.2.A-11/1/KONV-2012-0047 is acknowledged.

References

[1] J. Wang, J. Lu, S.B. Hočevar, P.A.M. Farias, B. Ogorevc, Anal. Chem. 72 (2000) 3218–3222.
[2] S.B. Hočevar, I. Švancara, B. Ogorevc, K. Vytřas, Anal. Chem. 79 (2007) (8693-8643).
[3] M. Korolczuk, K. Tyszczuk, M. Grabarczyk, Talanta 72 (2007) 957–961.
[4] I. Švancara, C. Prior, S.B. Hočevar, J. Wang, Electroanalysis 22 (2010) 1405–1420.
[5] A. Economou, Trends Anal. Chem. 24 (2005) 334–340.
[6] A. Królicka, A. Bobrowski, K. Kalcher, J. Mocák, I. Švancara, K. Vytřas, Electroanalysis 15 (2003) 1859–1863.
[7] A. Królicka, R. Pauliukaitė, I. Švancara, R. Metelka, E. Norkus, A. Bobrowski, K. Kalcher, K. Vytřas, Electrochem. Commun. 4 (2002) 193–196.
[8] K. Vytřas, I. Švancara, R. Metelka, Electroanalysis 14 (2002) 1359–1364.
[9] G. Kefala, A. Economou, A. Voulgaropoulos, M. Sofoniou, Talanta 61 (2003) 603–610.
[10] C.E. Banks, J. Kruusma, R.R. Moore, P. Tomcik, J. Peters, J. Davis, Š. Komorsky-Lovric, R.G. Compton, Talanta 65 (2005) 423–429.
[11] K.E. Toghill, G.G. Wildgoose, A. Moshar, C. Mulcahy, R.G. Compton, Electroanalysis 20 (2008) 1731–1737.
[12] I. Švancara, L. Baldrianová, M. Vlček, R. Metelka, K. Vytřas, Electroanalysis 17 (2005) 120–126.
[13] M.A. Baldo, S. Daniele, C. Bragato, J. Phys. IV (Proceedings) 107 (2003) 103–106.
[14] A. Królicka, A. Bobrowski, Electrochem. Commun. 6 (2004) 99–104.
[15] C. Kokkinos, A. Economou, Talanta 84 (2011) 696–701.
[16] L. Baldrianová, P. Agrafiotou, I. Švancara, A.D. Jannakoudakis, S. Sotiropoulos, J. Electroanal. Chem. 660 (2011) 31–36.
[17] L. Baldrianová, I. Švancara, S. Sotiropoulos, Anal. Chim. Acta 599 (2007) 249–255.
[18] R. Pauliukaitė, R. Metelka, I. Švancara, A. Królicka, A. Bobrowski, K. Vytřas, E. Norkus, K. Kalcher, Anal. Bioanal. Chem. 374 (2002) 1155–1158.
[19] A. Mardegan, S. Dal Borgo, P. Scopece, L.M. Moretto, S.B. Hočevar, P. Ugo, Electrochem. Commun. 24 (2012) 28–31.
[20] Gy.-Ja. Lee, Ch.K. Kim, M.K. Lee, Ch.K. Rhee, J. Electrochem. Soc. 157 (2010) J241–J244.
[21] C. Gouveia-Caridade, R. Pauliukaité, C.M.A. Brett, Electroanalysis 18 (2006) 854–861.
[22] L. Baldrianová, I. Švancara, A. Economou, S. Sotiropoulos, Anal.Chim. Acta 580 (2006) 24–31.
[23] H. Xu, L. Zeng, D. Huang, Y. Xian, L. Jin, Food Chem. 109 (2008) 834–839.
[24] G. Kefala, A. Economou, A. Voulgaropoulos, Analyst 129 (2004) 1082–1090.
[25] F. Torma, M. Kádár, K. Tóth, E. Tatár, Anal. Chim. Acta 619 (2008) 173–182.
[26] S. Chuanuwatanakul, W. Dungchai, O. Chailapakul, S. Motomizu, Anal. Sci. (Jpn) 24 (2008) 589–594.
[27] K. Keawkim, S. Chuanuwatanakul, O. Chailapakul, S. Motomizu, Food Control 31 (2013) 14–21.
[28] V. Guzsvány, H. Nakajima, N. Soh, K. Nakano, I. Švancara, K. Vytřas, L. Bjelica, T. Imato, Electroanalysis 23 (2011) 1593–1601.
[29] M. Stočes, I. Švancara, Int. J. Electrochem. Sci. 8 (2013) 5657–5671.
[30] H. Sopha, L. Baldrianová, E. Tesařová, G. Grincienė, T. Weidlich, I. Švancara, S. B. Hočevar, Electroanalysis 22 (2010) 1489–1493.
[31] C. Kokkinos, A. Economou, I. Raptis, C.E. Efstathiou, T. Speliotis, Electrochem. Commun. 9 (2007) 2795–2800.
[32] V. Guzsvány, K. Kádár, F. Gaál, L. Bjelica, K. Tóth, Electroanalysis 18 (2006) 1363–1371.
[33] V. Guzsvány, K. Kádár, Z.s. Papp, F. Gaál, L. Bjelica, K. Tóth, Electroanalysis 20 (2008) 291–300.
[34] V. Guzsvány, Zs. Papp, J. Zbiljić, O. Vajdle, M. Rodić, Molecules 16 (2011) 4451–4466.
[35] D. Deýlová, V. Vyskočil, A. Economou, V. Mansfeldová, J. Barek, Int. J. Electrochem. Sci. 9 (2014) 4653–4664.
[36] G.L. Kreft, O.C. De Braga, A. Spinelli, Electrochim. Acta 83 (2012) 125–132.
[37] C.A. De Lima, A. Spinelli, Electrochim. Acta 107 (2013) 542–548.
[38] A. Królicka, A. Bobrowski, J. Zareogonekbski, I. Tesarowicz, Electroanalysis 26 (2014) 756–765.
[39] N. Lezi, A. Economou, P.A. Dimovasilis, P.N. Trikalitis, M.I. Prodormidis, Anal. Chim. Acta 728 (2012) 1–8.
[40] P.A. Dimovasilis, M.I. Prodromidis, Anal. Chim. Acta 769 (2013) 49–55.
[41] V. Urbanová, M. Bartoš, K. Vytřas, A. Kuhn, Electroanalysis 22 (2010) 1524–1530.
[42] T. Romann, E. Lust, Electrochim. Acta 55 (2010) 5746–5752.
[43] C. Chen, X. Niu, Y. Chai, H. Zhao, M. Lan, Sens. Actuators B: Chem 178 (2013) 339–342.
[44] A.P. Periasamy, S. Yang, S.M. Chen, Talanta 15 (2011) 15–23.
[45] Y. Wang, D. Pan, X. Li, W. Qin, Chin. J. Chem. 27 (2009) 2385–2391.
[46] G.D. Liu, Y.H. Lin, Y. Tu, Z.F. Ren, Analyst. 130 (2005) 1098.
[47] G.H. Hwang, W.K. Han, J.S. Park, S.G. Kang, Talanta 76 (2008) 301–308.
[48] H. Xu, L. Zeng, S. Xing, Y. Xian, G. Shi, L. Jin, Electroanalysis 20 (2008) 2655–2662.
[49] W. Deng, Y. Tan, Q. Xie, Y. Li, X. Liang, S. Yao, Electroanalysis 21 (2009) 2477–2485.
[50] N. Pikroh, P. Vanalabhpatana, ECS Trans. 45 (2013) 39–46.
[51] N. Wang, X. Dong, Anal. Lett. 41 (2008) 1267–1278.
[52] K.B. Wu, S.S. Hu, J.J. Fei, W. Bai, Anal. Chim.Acta 489 (2003) 215–221.
[53] J. Rajeev, Dhanjai, J. Electrochem. Soc. 161 (2014) H29–H35.
[54] J. Rajeev, Dhanjai, S. Sharma, Colloids Surf. A: Physicochem. Eng. Aspects 436 (2013) 178–184.
[55] M. Taillefert, B.J. MacGregor, J.F. Gaillard, C.P. Lienemann, D. Perret, D.A. Stahl, Environ. Sci. Technol. 36 (2002) 468–476.
[56] S. Daniele, C. Bragato, M.A. Baldo, Anal. Chim. Acta 346 (1997) 145–156.
[57] S. Daniele, C. Bragato, M.A. Baldo, J. Wang, J. Lu, Analyst 125 (2000) 731–735.
[58] A. Bertolin, G.A. Mazzocchin, D. Rudello, P. Ugo, Mar. Chem. 59 (1997) 127–140.
[59] G.W. Luther III, C.E. Reimers, D.B. Nuzzio, D. Lovalvo, Environ. Sci. Technol. 33 (1999) 4352–4356.
[60] M. Taillefert, C.F. Hover, F.T. Rozan, M.S. Theberge, G.W. Luther, Estuaries 25 (2002) 1088–1096.
[61] P. Ugo, F. Cavalieri, D. Rudello, L.M. Moretto, E. Argese, Sensors 1 (2001) 102–113.
[62] A. Bobrowski, P. Kapturski, J. Zarebski, J. Dominik, D.A.L. Vignati, Anal. Lett. 45 (2012) 495–507.
[63] M. Taillefert, G.W. Luther III, D.B. Nuzzio, Electroanalysis 12 (2000) 401–412.
[64] D.M. Di Toro, C.S. Zarba, D.J. Hansen, W.J. Berry, R.C. Swartz, C.E. Cowan, S.P. Pavlou, H.E. Allen, T.N.A. Thomas, P.R. Paquinand, W.J. Berry, Environ. Toxicol. Chem. 10 (1991) 1541–1583.

[65] A.M. Ashrafi, S. Cerovac, S. Mudrić, V. Guzsvány, L. Husáková, I. Urbanová, K. Vytřas, Sens. Actuators B: Chem 191 (2013) 320–325.
[66] M. Endo, K. Takeuchi, T. Hiraoka, T. Furuta, T. Kasai, X. Sun, C.H. Kiang, M.S. Dresselhaus, J. Phys. Chem. Solids 58 (1997) 1707–1712.
[67] Uredba o graničnim vrednostima zagađujućih materija u površinskim i podzemnim vodama i sedimentu i rokovim za njihovo dostizanje, Prilog 3. Sediment, "Službeni glasnik RS", No. 50/2012.